

Response of 100% Internal Carrier Collection Efficiency Silicon Photodiodes to Low-Energy Ions

Herbert O. Funsten, *Member, IEEE*, Stephen M. Ritzau, Ronnie W. Harper, and Raj Korde, *Member, IEEE*

Abstract—We measure the response of silicon photodiodes to irradiation by H^+ , He^+ , C^+ , N^+ , O^+ , Ne^+ , and Ar^+ ions with energies up to 60 keV. The unique properties of these photodiodes, including an ultrathin SiO_2 dead layer and 100% internal carrier collection efficiency, allow direct measurement of the total energy lost to nuclear (nonionizing) and electronic (ionizing) energy loss processes, which are important for quantifying effects such as damage and charge deposition. When plotted as a function of $E/mZ^{1/2}$, where E , m , and Z are the incident ion energy, mass, and atomic number, respectively, the responsivity is found to follow a single curve that represents all ion species and energies used in this study. This enables rapid, accurate estimation of damage and charge deposition by an ion as a function of penetration depth in silicon. A comparison of the measurements with the stopping and range of ions in matter (SRIM) Monte Carlo simulation code shows that SRIM significantly overestimates the fraction of the incident energy lost to electronic stopping processes for $E/mZ^{1/2} < 2$ keV/amu.

Index Terms—Electronic energy loss, ion radiation, ionizing radiation, nuclear energy loss, photodiodes, radiation effects, silicon detectors.

I. INTRODUCTION

SILICON p-n junction photodiodes with 100% internal carrier collection efficiency are used as absolute and transfer standards for measurement of extreme ultraviolet (EUV) photons [1], [2]. These photodiodes can be employed, for example, to measure EUV in fusion, space, and laboratory plasma research. Due to the thin (~ 60 Å SiO_2) passivation layer of the detectors, ions with a minimum energy of several hundred eV can transit this thin dead region and induce a signal in the photodiode. This signal can be an unwanted background in an EUV measurement, or it could be used to detect the ions themselves. To quantify the signal induced by these ions, we characterize the photovoltaic response of the photodiodes to irradiation by ions at incident energies less than 60 keV.

In addition to measurement of the response of these photodiodes for their use in plasma environments, the unique character-

istics (thin dead layer and 100% internal carrier collection efficiency) of these photodiodes have allowed the fortuitous, quantitative measurement of the energy lost by an incident ion to electronic stopping processes (electronic excitation and ionization) and to nuclear stopping processes (Coulombic collisions with target nuclei) for slow ions. A systematic understanding of these energy loss processes for different ion-energy combinations is important for assessing and predicting a variety of effects in silicon such as the magnitude of the charge pulse generated by an ion, radiation-enhanced diffusion [3], [4], and device damage, which is strongly correlated with nuclear stopping processes [5]–[10].

Solid-state detectors offer a direct method for studying the energy lost to electronic stopping processes since this energy loss is proportional to the measured output pulse magnitude. However, these measurements at best provide only a lower bound of the energy lost to electronic stopping processes. Quantitative measurements by solid-state detectors operated in single particle detection mode are particularly onerous at low energies for two primary reasons. First, the small pulse magnitude results in a low signal-to-noise ratio that makes quantification of the mean pulse magnitude per incident ion difficult. Second, the pulse-height defect renders the measurement ambiguous. The pulse-height defect is the deviation of the measured responsivity from the ideal responsivity of 0.27 A/W (for Si) that would be observed if all of the ion energy went into electron-hole pair creation and all of the electron-hole pairs were measured. The three components of the pulse-height defect are [11]–[14] 1) energy loss by the ion in the dead layer that does not contribute to the output signal, 2) recombination of electron-hole pairs either along the ion track (negligible for slow ions due to the low density of the plasma along the ion track [15], [16]) or at defect sites within the device, and 3) energy lost through nuclear (nonionizing) stopping processes that do not generate electron-hole pairs.

The energy lost in the dead layer of a conventional solid-state detector can be modeled with reasonable accuracy at high energies; however, at low energies, the dead layer energy loss can become a substantial fraction of the total energy lost by the ion in the device, so an error in the model will significantly impact the accuracy of the measurement. Furthermore, the energy lost to electronic and nuclear stopping in the active region and the apparent energy lost due to recombination at defects within the device are extremely difficult to separate.

The unique properties of the devices used in this study enable accurate measurement of the energy lost to nuclear stopping processes for three reasons. First, the devices have no intrinsic recombination of electron-hole pairs [17]. Second, the 60 Å SiO_2

Manuscript received July 17, 2001. The work at Los Alamos National Laboratory was performed under the auspices of the U.S. Department of Energy, and was supported by NASA under Grant W-19,866. The work at International Radiation Detectors was supported in part by the U.S. Department of Energy under Grant DE-FG03-96ER82190.

H. O. Funsten and R. W. Harper are with Los Alamos National Laboratory, Los Alamos, NM 87545 USA (e-mail: hfunsten@lanl.gov; rharper@lanl.gov).

S. M. Ritzau was with Los Alamos National Laboratory, Los Alamos, NM 87545 USA. He is now with ON Semiconductor, East Greenwich, RI 02818 USA (e-mail: Stephen.ritzau@onsemi.com).

R. Korde is with International Radiation Detectors, Torrance, CA 90505 USA (e-mail: irdinc@earthlink.net).

Publisher Item Identifier S 0018-9499(01)10531-9.

dead layer is extremely thin (approximately ten times less than conventional solid-state detectors), so errors in modeling the energy lost in this layer are correspondingly smaller. Third, the devices are operated in photocurrent mode, so the large signal induced in the device by the ion beam is much larger than the dark current, enabling accurate signal-to-noise measurements. We exploit these unique properties to quantify the total energy lost to nuclear and electronic stopping, and we compare these measurements to the Monte Carlo simulation code “Stopping and Range of Ions in Matter” (SRIM) [18].

II. EXPERIMENT

The experiment, similar to that used to characterize the response of the same detectors to electrons [19] and the damage induced by slow ions [20], involved exposing a 6-mm-diameter spot on the photodiodes to ion beams of H^+ , He^+ , C^+ , N^+ , O^+ , Ne^+ , and Ar^+ at energies E less than or equal to 60 keV (see top panel of Fig. 1). The ion beam current I_{BEAM} was measured before and after irradiation of the photodiode to ensure that the beam current did not drift. Additionally, the mean dark current I_D was measured before and after each irradiation. The photodiode current I_{PD} generated by the ion beam was measured during irradiation. Typically, I_{PD} was ~ 50 nA, which was much greater than the typical dark current of ~ 10 pA. The photodiode responsivity is

$$R = (I_{PD} - I_D)/(TI_{BEAM}E) \quad (1)$$

where T is the transmission probability of the incident ions through the 60 Å SiO_2 dead layer of the photodiode as calculated using SRIM [18]. The SRIM calculations were performed by tracking both the number of ions transmitted through a 60 Å SiO_2 foil and the mean energy of the transmitted ions. Inclusion of the transmission probability T accounts for ions that are completely stopped in the foil, or dead layer. This is a significant correction for heavy, slow ions (e.g., T equals 11% for 1 keV He^+ , 5% for 5 keV C^+ , 12% for 5 keV Ne^+ , and 5% for 10 keV Ar^+). Equation (1) does not correct for energy loss in the SiO_2 dead layer; instead, this energy loss is treated as an error in the initial energy E , and the magnitude of this error equals the mean energy loss through the SiO_2 foil calculated by SRIM.

The unbiased n-p silicon photodiodes used in this experiment had a 60 Å SiO_2 dead layer. These diodes are known to have 100% carrier collection efficiency for 650-nm photons [2], [17]. Since the penetration depth of these photons in silicon is approximately 20 μm , we reasonably assume that these diodes will have complete electron-hole pair collection up to this depth when the carriers are generated by any particles, including ions. The top panel of Fig. 1 shows the projected ranges of the different ions in the photodiode at the energies used in this study (the minimum and maximum incident energy are labeled for each ion species). The projected ranges, which were calculated using SRIM with a Si target having a 60 Å SiO_2 entrance layer, are less than 1 μm , so the device should have 100% carrier collection efficiency for this study.

Fig. 1 shows the computed potential diagram of the device using SGFramework [21] based on the doping profile. Electrons generated in the active region of the device drift toward

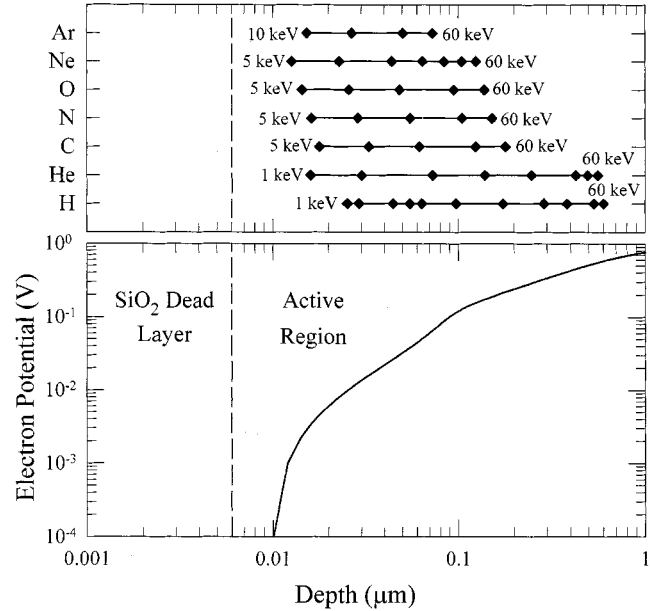


Fig. 1. The top panel shows the mean projected range of the ions in the photodiodes based on SRIM calculations [18] for the energies of the incident ion species used in this study (diamond symbols). The bottom panel is the electron potential of the devices computed using the doping profile and SGFramework [21]. Electrons generated in the active layer of the device drift toward the surface due to the intrinsic electric field, and the charge subsequently diffuses toward the perimeter contacts within a narrow planar channel located near the Si- SiO_2 interface.

a narrow channel adjacent to the Si- SiO_2 interface and are diffusively transported to the contacts on the device perimeter.

III. RESULTS

Fig. 2 shows the measured photodiode responsivity R as a function of the ion beam energy E for the ions used in this study. The error bars to the left of the data points represent the mean energy lost by the incident ions in the SiO_2 dead layer calculated using SRIM. The length of an error bar corresponds to the energy deposited in the SiO_2 layer. However, there are two ways in which this energy deposited in the dead layers can still contribute to the measured signal. First, the incident ion can generate Si or O recoils in the dead layer. From first principles, the initial recoil is forward-scattered toward the active region; furthermore, the net velocity of a collision cascade will also be directed toward the active region [22]. Therefore, the recoil (or collision cascade) generated in the dead layer can deposit energy in the active region through electronic stopping processes that result in electron-hole pair creation.

Second, electron-hole pairs are generated in the SiO_2 , although at a lower rate than for silicon due to the large SiO_2 electron-hole pair creation energy of ~ 17 eV [23], [24]. These electron-hole pairs can diffuse to the active region, where they are collected and measured. This effect was observed in experiments in which low-energy incident electrons, which should not penetrate the SiO_2 layer, generated a significant response in the photodiodes [19]. A similar effect was observed in photodiodes exposed to photons that are strongly absorbed in the SiO_2 [17].

The cumulative fraction f_E of an ion's incident energy E lost to electronic stopping processes is $f_E = E_{e-h}R$, where

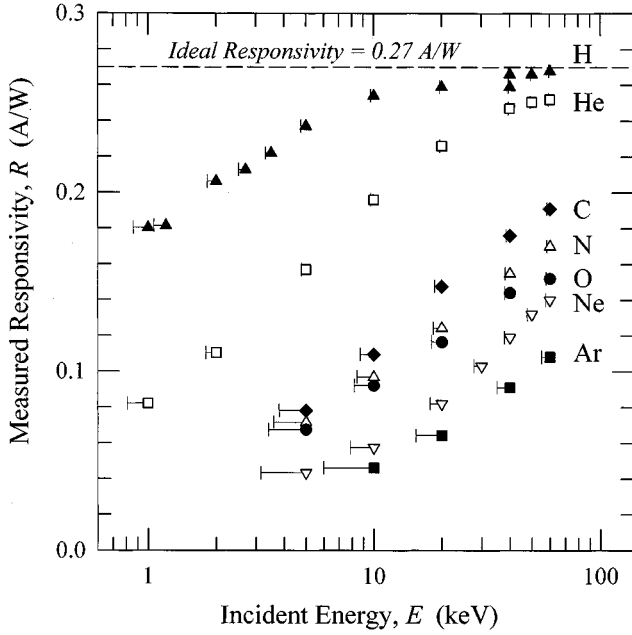


Fig. 2. The measured responsivity R is shown as a function of incident ion energy for different ion species. The dashed line corresponds to the ideal responsivity equal to 0.27 A/W for Si that would be observed if all of the incident ion energy was deposited into electron-hole pair creation in the active region of the device. Deviation from this ideal value is the result of energy lost to nuclear stopping processes by both the primary ion and silicon recoils. The error bars to the left of the data points represent the mean energy lost in the 60 Å SiO_2 dead layer by ions transmitted through this layer calculated using SRIM [18].

E_{e-h} is the mean energy required for electron-hole pair formation ($E_{e-h} = 3.7$ eV in silicon [25]). If all of the initial energy lost by the ions went into formation of electron-hole pairs in the active region, then the responsivity would equal 0.27 A/W and $f_E = 1$. This “ideal” case is shown as the dashed line in Fig. 2. For most of the measurements, the measured responsivity lies significantly below the ideal responsivity, and this difference ΔR increases with increasing ion mass and decreasing ion energy.

Before proceeding further, we must clarify the complex nature of the physical processes that are being measured. An incident ion loses a fraction of its energy directly to nuclear (f_N^P) and electronic (f_E^P) stopping processes, where of course $f_N^P + f_E^P = 1$ (the superscript P denotes the primary ion). Kinetic energy is transferred to silicon nuclei through nuclear stopping, and these recoiling Si atoms lose their energy to both nuclear and electronic processes. Therefore, energy lost by the incident ion to nuclear stopping processes can subsequently be converted to energy lost by electronic stopping processes by Si recoils. By additionally considering the energy loss processes of Si recoils, the fraction f_N^P of energy lost by the incident ion to nuclear stopping processes overestimates the total energy lost to nuclear stopping processes.

Using a simplistic representation, we average the energy loss processes of the entire distribution of Si recoils and define f_N^{Si} and f_E^{Si} as the fractions of energy lost by these recoils to nuclear and electronic stopping processes, respectively, and $f_N^{\text{Si}} + f_E^{\text{Si}} = 1$. We note that f_N^{Si} includes the displacement energy of the Si recoils.

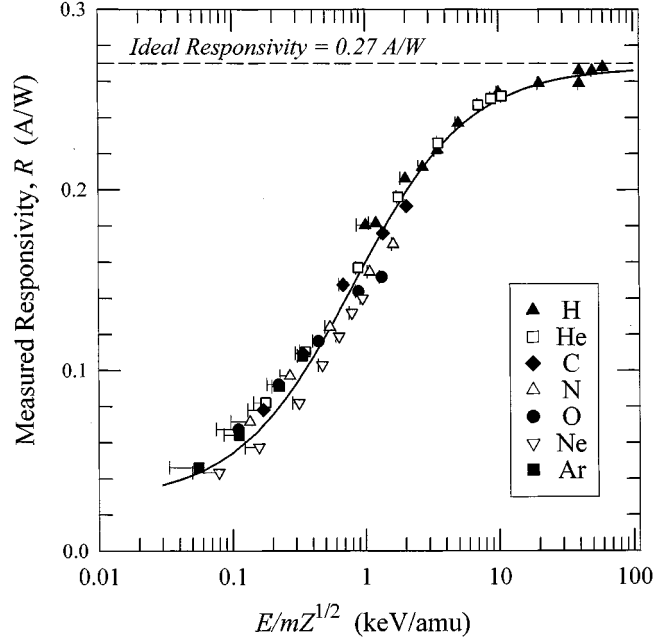


Fig. 3. When plotted as a function of $E/mZ^{1/2}$, the measured responsivity R of the various ions and energies fall approximately on a single curve. The solid line is an empirical fit to the data [see (2)]. This systematic variation of the responsivity enables simple estimation of the total energy lost to electronic and nuclear stopping processes. The error bars represent the mean energy lost in the SiO_2 dead layer, similar to Fig. 2.

The total energy deposited by the incident ion is partitioned into nuclear and electronic energy loss processes according to

$$E = E f_E^P + E f_N^P (f_E^{\text{Si}} + f_N^{\text{Si}}) \quad (2)$$

where, as before, E is the incident ion energy. The cumulative fractions of the incident ion energy lost to electronic and nuclear stopping processes are

$$f_E = f_E^P + f_N^P f_E^{\text{Si}} \quad (3)$$

$$f_N = f_N^P f_N^{\text{Si}}. \quad (4)$$

The measured responsivity is $R = (f_E/E_{e-h})$ and the difference ΔR between the ideal responsivity of 0.27 A/W and R is $\Delta R = (f_N/E_{e-h})$. These measurements therefore provide a quantitative evaluation of the total energy lost to nuclear stopping processes relative to the total energy lost to electronic stopping processes.

A. Universal Representation of the Responsivity

Fig. 3 shows the measured responsivity as a function of $E/mZ^{1/2}$, where m and Z are the incident ion mass and atomic number, respectively. We have used the isotopic incident ion species ${}^3\text{He}^+$ and ${}^4\text{He}^+$ to establish the $Z^{1/2}$ dependence. By defining $\varepsilon = (E/mZ^{1/2})$, we find that the data generally fall along a single universal curve that can be empirically fitted to

$$R(\varepsilon) = (0.03 + 0.33\varepsilon)/(1 + 1.22\varepsilon) \quad (5)$$

where ε and $R(\varepsilon)$ are expressed in units of keV/amu and A/W, respectively. From $R(\varepsilon)$ we obtain a universal representation of the fraction of the total energy lost to electronic stopping $f_E(\varepsilon) = 3.7R(\varepsilon)$ and the fraction of the total energy lost to

nuclear stopping $f_N(\varepsilon) = 1 - f_E(\varepsilon)$. The total energy lost to electronic stopping processes is equal to the total energy lost to nuclear stopping processes (i.e., $f_E(\varepsilon) = f_N(\varepsilon) = 0.5$) at $\varepsilon = 0.64$ keV/amu.

Note in particular the significant overlap of the responsivity of He^+ , a light ion, with that of Ar^+ , a heavy ion, showing an important systematic trend in the data that spans a large difference in atomic number. In addition to using these data to quantify the response of these photodiodes to ion irradiation, we can use this curve to predict important ion-induced processes in silicon: electron-hole pair creation rate and total damage due to nuclear stopping processes.

We furthermore note that extrapolation to higher energies (>2 keV/amu) of the 40 and 60 keV C, N, and O data shown in Fig. 3 indicates a systematic and significant deviation from the fitted line. At these higher energies, the nuclear stopping power rapidly decreases so that the total energy lost to nuclear stopping approaches a constant value that is independent of energy but dependent on mass. The apparent deviation of the data if extrapolated to higher energies likely reflects the mass dependence of this constant.

B. Comparison With SRIM

The semi-empirical SRIM computer code [18] is routinely used for simulating the kinetics of ion interactions in solids [8], [26], [27] and is often regarded as a standard for gauging the accuracy of particle-solid interaction models. We have used SRIM in the “full damage cascade mode” that follows every Si recoil until its energy falls below the displacement energy of Si atoms from the lattice (~ 15 eV). For each of these Monte Carlo simulations, the fraction $f_{E,\text{SRIM}}$ of energy lost to ionizations by both the incident ion and recoil atoms was computed.

Fig. 4 shows the ratio of $f_{E,\text{SRIM}}$ to the fraction f_E of energy lost to electronic stopping derived from the responsivity data in Fig. 3. The data substantially disagree with SRIM at the smallest values of $E/mZ^{1/2}$ used in this study but converge toward agreement with SRIM ($f_{E,\text{SRIM}}/f_E = 1$) with increasing $E/mZ^{1/2}$. For $E/mZ^{1/2} > 2$ keV/amu, the agreement suggests that the total energies lost to electronic and nuclear stopping processes are correctly partitioned at higher energies by SRIM. For reference, the measured f_E for the heavy ions is approximately 20–25% at $E/mZ^{1/2} = 0.1$ keV/amu. An interesting deviation is observed for He^+ , which follows the same general trend as the H^+ data except that it agrees with SRIM down to a value of $E/mZ^{1/2}$ that is approximately five times lower than for H^+ .

SRIM significantly overestimates the amount of total energy lost to electronic stopping processes for $E/mZ^{1/2} < 2$ keV/amu, and this overestimation increases nearly linearly with decreasing $E/mZ^{1/2}$ to a value of almost 3 at 0.1 keV/amu. Several studies agree with these results. For example, [28] found a consistent 15% underestimation by SRIM of the range and range straggling of Er and Yb in Si at $E/mZ^{1/2}$ ranging from 0.28 to 3.81 keV/amu. The experimental results were compared with simulations using the IMSIL Monte Carlo code [29] in which a correction factor to the electronic stopping was employed. The comparison showed an enormous overestimation of electronic stopping at 0.28 keV/amu and a moderate

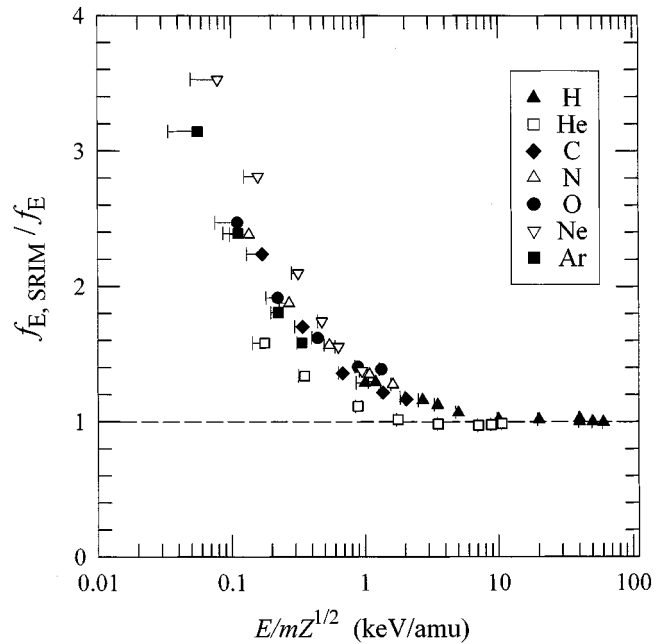


Fig. 4. By multiplying the responsivity R by the energy $E_{e-h} = 3.7$ eV required to create an electron-hole pair in Si, we obtain the fraction f_E of an ion's initial energy lost to electronic stopping (ionizing) processes by both the primary ion and recoils. The figure shows the ratio of $f_{E,\text{SRIM}}$ determined by SRIM to the measured f_E as a function of $E/mZ^{1/2}$. The error bars represent the energy lost by the incident ion in the SiO_2 dead layer, similar to Figs. 2 and 3.

overestimation of electronic stopping at 3.8 keV/amu. Using range experiments of Au incident on Si at $E/mZ^{1/2}$ ranging from 0.7 to 1.7, [30] also found a substantial overestimation by SRIM of the electronic stopping power.

The underestimation of the projected range by SRIM for slow, heavy ions in light targets has been attributed to a correlation between nuclear and electronic stopping that is not included in SRIM [31]–[33]. While SRIM results and the range observations agree closely when this correlation is included, the correlation term results in a *reduction* of the nuclear stopping power, a net decrease in the stopping power, and an increase in ion range. In contrast, the present results suggest that the nuclear stopping component is underestimated by SRIM rather than overestimated.

IV. CONCLUSION

Nuclear stopping processes have a direct impact on radiation damage, whereas electronic stopping processes generate charge in a device that is the source of radiation-enhanced diffusion, which can result in damage annealing. To date, experiments such as comparing range measurements to theory have indirectly inferred the partitioning of these stopping processes at low energies for which nuclear stopping cannot be ignored.

Measurement of the response of thin window, 100% internal carrier collection efficiency photodiodes described in this study has fortuitously allowed the direct quantification of the fraction of the total ion energy lost to nuclear and electronic stopping processes. Using a scaling factor of $E/mZ^{1/2}$, the responsivity data (and therefore the fraction of energy lost to electronic or nuclear stopping) fall on a single curve for all ion energies and species used in this study. This dependence can be used for a

reasonably accurate estimation of the total energy lost to nuclear or electronic stopping processes. When the data are compared to SRIM calculations, SRIM is observed to systematically overestimate the fraction of the total energy lost to electronic stopping processes for $E/mZ^{1/2} < 2$ keV/amu, although the data converge toward agreement with SRIM for $E/mZ^{1/2} > 2$.

ACKNOWLEDGMENT

The authors gratefully acknowledge the laboratory assistance of J. Baldonado and D. Everett.

REFERENCES

- [1] R. Korde, J. S. Cable, and L. R. Canfield, "One gigarad passivating nitrided oxides for 100% internal quantum efficiency silicon photodiodes," *IEEE Trans. Nucl. Sci.*, vol. 40, no. 6, pp. 1655–1659, 1993.
- [2] K. W. Wenzel, C. K. Lick, D. A. Pappas, and R. Korde, "Soft x-ray silicon photodiode with 100% quantum efficiency," *IEEE Trans. Nucl. Sci.*, vol. 41, no. 4, pp. 979–983, 1994.
- [3] D. V. Lang and L. C. Kimmerlin, "Observation of recombination-enhanced defect reactions in semiconductors," *Phys. Rev. Lett.*, vol. 33, no. 8, pp. 489–492, 1974.
- [4] E. L. Hu, C.-H. Chen, and D. L. Green, "Low-energy ion damage in semiconductors: A progress report," *J. Vac. Sci. Technol. B*, vol. 14, no. 6, pp. 3632–3636, 1996.
- [5] G. P. Summers, E. A. Burke, C. J. Dale, E. A. Wolicki, P. W. Marshall, and M. A. Gehlhausen, "Correlation of particle-induced displacement damage in silicon," *IEEE Trans. Nucl. Sci.*, vol. NS-34, no. 6, pp. 1134–1139, 1987.
- [6] G. P. Summers, E. A. Burke, P. Shapiro, S. R. Messenger, and R. J. Walters, "Damage correlations in semiconductors exposed to gamma, electron, and proton radiation," *IEEE Trans. Nucl. Sci.*, vol. 40, no. 6, pp. 1372–1379, 1993.
- [7] M. Kurokawa, T. Motobayashi, K. Shimoura, H. Murakami, Y. Ikeda, S. Moriya, Y. Yanagisawa, and T. Nomura, "Radiation damage factor for ion-implanted silicon detectors irradiated with heavy ions," *IEEE Trans. Nucl. Sci.*, vol. 42, no. 3, pp. 163–166, 1995.
- [8] S. R. Messenger, E. A. Burke, G. P. Summers, M. A. Xapsos, R. J. Walters, E. M. Jackson, and B. D. Weaver, "Nonionizing energy loss (NIEL) for heavy ions," *IEEE Trans. Nucl. Sci.*, vol. 46, no. 6, pp. 1595–1602, 1999.
- [9] E. H. Lee, "Ion-beam modification of polymeric materials: Fundamental principles and applications," *Nucl. Instrum. Meth. B*, vol. 151, pp. 29–41, 1999.
- [10] J. R. Srour and D. H. Lo, "Universal damage factor for radiation-induced dark current in silicon devices," *IEEE Trans. Nucl. Sci.*, vol. 47, no. 6, pp. 2451–2459, 2000.
- [11] E. C. Finch and A. L. Rodgers, "Measurements of the pulse height defect and its mass dependence for heavy-ion silicon detectors," *Nucl. Instrum. Meth.*, vol. 113, pp. 29–40, 1973.
- [12] W. N. Lennard, H. Geissel, K. B. Winterbon, D. Phillips, T. K. Alexander, and J. S. Forster, "Nonlinear response of Si detectors for low-Z ions," *Nucl. Instrum. Meth. A*, vol. 248, pp. 454–460, 1986.
- [13] M. Ogihara, Y. Nagashima, W. Galster, and T. Mikumo, "Systematic measurements of pulse height defects for heavy ions in surface-barrier detectors," *Nucl. Instrum. Meth. A*, vol. 251, pp. 313–320, 1986.
- [14] G. Pasquali, G. Casini, M. Bini, S. Calamai, A. Olmi, G. Poggi, A. A. Stefanini, F. Saint-Laurent, and J. C. Steckmeyer, "Pulse height defect of energetic heavy ions in ion-implanted Si detectors," *Nucl. Instrum. Meth. A*, vol. 405, pp. 39–44, 1998.
- [15] E. C. Finch, M. Asghar, and M. Forte, "Plasma and recombination effects in the fission fragment pulse height defect in a surface barrier detector," *Nucl. Instrum. Meth.*, vol. 163, pp. 467–477, 1979.
- [16] C. F. G. Delaney and E. C. Finch, "Rise and plasma times in semiconductor-detectors," *Nucl. Instrum. Meth.*, vol. 215, pp. 219–223, 1983.
- [17] R. Korde and J. Geist, "Quantum efficiency stability of silicon photodiodes," *Appl. Opt.*, vol. 26, no. 24, pp. 5284–5290, 1987.
- [18] J. F. Ziegler, J. P. Biersack, and U. Littmark. (1985) *Stopping and Range of Ions in Solids*
- [19] H. O. Funsten, D. M. Suszcynsky, S. M. Ritzau, and R. Korde, "Response of 100% internal quantum efficiency silicon photodiodes to 200 eV to 40 keV electrons," *IEEE Trans. Nucl. Sci.*, vol. 44, pp. 2561–2565, Dec. 1997.
- [20] S. M. Ritzau, H. O. Funsten, R. W. Harper, and R. Korde, "Damage induced by 10–60 keV ion irradiation in 100% internal carrier collection efficiency silicon photodiodes," *IEEE Trans. Nucl. Sci.*, vol. 45, pp. 2820–2925, 1998.
- [21] K. M. Kramer and W. N. G. Highton, *Semiconductor Devices: A Simulation Approach*. Upper Saddle River, NJ: Prentice-Hall, 1998.
- [22] M. W. Scklerl, M. Vicanek, and P. Sigmund, "Momentum in atomic collision cascades," *Nucl. Instrum. Meth. B*, vol. 102, pp. 86–92, 1995.
- [23] G. A. Ausman and F. B. McLean, "Electron-hole pair creation energy in SiO₂," *Appl. Phys. Lett.*, vol. 26, no. 4, pp. 173–175, 1975.
- [24] J. M. Benedetto and H. E. Boesch, "The relationship between ⁶⁰Co and 10-keV damage in MOS devices," *IEEE Trans. Nucl. Sci.*, vol. NS-33, no. 6, pp. 1318–1323, 1986.
- [25] C. J. Wu and D. B. Wittry, "Investigation of minority-carrier diffusion lengths by electron bombardment of Schottky barriers," *J. Appl. Phys.*, vol. 49, no. 5, pp. 2827–2836, 1978.
- [26] V. Zajic and P. Thieberger, "Heavy ion linear energy transfer measurements during single event upset testing of electronic devices," *IEEE Trans. Nucl. Sci.*, vol. 46, no. 1, pp. 59–69, 1999.
- [27] G. S. Randhawa and H. S. Virk, "Stopping power and range of heavy ions in solids: A comparative study," *Rad. Meas.*, vol. 26, no. 4, pp. 541–560, 1996.
- [28] L. Palmethofer, M. Gritsch, and G. Hobler, "Range of ion-implanted rare earth elements in Si and SiO₂," *Mater. Sci. Eng. B*, vol. 81, pp. 83–85, 2001.
- [29] G. Hobler, "Monte Carlo simulation of two-dimensional implanted dopant distributions at mask edges," *Nucl. Instrum. Meth. B*, vol. 96, pp. 155–162, 1995.
- [30] Z. Yongjun, L. Xiting, Z. Tao, X. Zonghuang, and S. Dingyu, "Stopping power for MeV energy Au ions in silicon," *Nucl. Instrum. Meth. B*, vol. 135, pp. 128–131, 1998.
- [31] P. L. Grande, F. C. Zawislak, D. Fink, and M. Behar, "Range parameters study of medium-heavy ions implanted into light substrates," *Nucl. Instrum. Meth. B*, vol. 61, pp. 282–290, 1991.
- [32] M. Behar, P. L. Grande, R. Wagner de Oliveira, and J. P. Biersack, "Range parameters of heavy ions implanted into boron films," *Nucl. Instrum. Meth. B*, vol. 59, pp. 1–4, 1991.
- [33] G. Kuri, "Projected range and range straggling of MeV Au ions in Si," *Nucl. Instrum. Meth. B*, vol. 117, no. 3, pp. 213–217, 1996.